PROCEEDINGS OF SCIENCE

ONLINE ICRC 2021
THE ASTROPARTICLE PHYSICS CONFERENCE
Berlin | Germany
37th International Cosmic Ray Conference
12–23 July 2021

Simulation Study on Scaler Mode in LHAASO-KM2A

Zhicheng Huang[1], Daihui Huang,[1,*] Xunxiu Zhou[1], Jing Zhao[3], Huihai He[3], Songzhan Chen[3], Xinhua Ma[3], Dong Liu[4], Kegu Axi[1] and Bing Zhao[1] on behalf of the LHAASO Collaboration
(a complete list of authors can be found at the end of the proceedings)

[1]*School of Physical Science and Technology,Southwest Jiaotong University, Chengdu 610031,China*
[2]*Key Laboratory of Cosmic Rays, Ministry of Education, Tibet University, Lhasa 850000, China*
[3]*Institute of High Energy Physics,CAS,Beijing 100049,China*
[4]*Institute of Frontier and Interdisciplinary Science,Shandong University,Qingdao 266237,China*
E-mail: hdhamy@sina.com

Abstract. LHAASO, located at Daocheng in Sichuan province of China with an altitude up to 4410 m above the sea level, takes the function of hybrid technology to detect cosmic rays. As the major array of LHAASO, KM2A is composed of 5195 electromagnetic particle detectors (EDs) and 1188 muon detectors (MDs). In the ground-based experiments, there are two common independent data acquisition systems, corresponding to the scaler and shower operation modes. In order to learn more about the scaler mode in LHAASO-KM2A, we adopt the CORSIKA to study the shower development and employ the G4KM2A (based on Geant4) to simulate the detector responses. For one cluster (composed of 64 EDs) in the array of KM2A-ED, the event rates of showers having a number of fired EDs $\geq$ 1, 2, 3 and 4 (in a time coincidence of 100 ns) are recorded. The average rates of the four multiplicities are $\sim$ 88 kHz, $\sim$ 1.4 kHz, $\sim$ 210 Hz and $\sim$ 110 Hz, respectively. For the array of KM2A-MD, there are 16 MDs in one cluster. The average rates with multiplicities $\geq$ 1 and 2 are $\sim$ 84 kHz and $\sim$ 890 Hz, respectively. The corresponding primary energies are also given. According to our simulations, the energy threshold of the scaler mode can be lowered to $\sim$ 100 GeV. At the same time, the energy threshold of LHAASO-KM2A in shower mode is presented for comparison. The simulation results in this work are beneficial for the online trigger with scaler mode, and also be useful in understanding the experiment results in LHAASO-KM2A.

Keywords: Scaler mode; Shower mode; LHAASO-KM2A; Monte Carlo simulations; Cosmic rays

37th International Cosmic Ray Conference (ICRC 2021)
July 12th – 23rd, 2021
Online – Berlin, Germany

*Presenter

© Copyright owned by the author(s) under the terms of the Creative Commons Attribution-NonCommercial-NoDerivatives 4.0 International License (CC BY-NC-ND 4.0).

PoS(ICRC2021)365

1. Introduction

When a primary cosmic ray enters into the atmosphere, it will interact with the nucleus and others in the air, producing many new secondary particles via the hadron and electromagnetic cascades. These secondary particles are distributed in many kilometers wide like raining down, known as Extensive Air Shower (EAS). Because of carrying a lot of information related to primary cosmic rays, scientists often study the primary cosmic rays indirectly by analyzing the characteristics of the secondary particles in the EAS. The ground-based experiments (i.e. ARGO-YBJ [1], LHAASO [2]) have the advantages of lower cost and much larger sensitive area . It can provide a powerful experimental facility for observing cosmic rays.

There are two independent data acquisition systems in the ground-based experiment, corresponding to the shower and scaler operation modes [1,3]. In shower mode, when conditions are met to trigger the detector, the information on the arrival time and location of each hit are recorded, allowing the shower core, arrival direction and energy of the primary cosmic ray reconstruction. Using these reconstructed data, further research on γ-ray astronomy [1,4] and cosmic ray physics [5], can be done. In scaler mode, it is not necessary for too many detectors to be hit at the same time. The total counting rates of all the particles arriving at the detectors are recorded during a fixed time interval, which can greatly reduce the detector primary energy threshold [6, 7]. The scaler data can be used in searching for the transient events, such as gamma-ray bursts (GRBs) [8], GLE event and Forbush decreases [9] etc. By studying the variations of counting rates in this mode, the correlation between atmospheric electric field and the intensity changes of ground cosmic ray during thunderstorms can be studied [10,11].

Therefore, both shower mode and scaler mode for data acquisition are important in the ground-based cosmic ray experiments. Currently, the KM2A array only operates in shower mode. In this work, Monte Carlo simulations were performed to study the performance of scaler mode in the KM2A array.

2. LHAASO-KM2A

The High Altitude Cosmic Ray Observatory (LHAASO), a project under the construction at Daocheng (4410 m a.s.l., Sichuan, China), consists of three sub-arrays: an area of 1.3 km^2 array (KM2A), a 78,000 m^2 water Cherenkov detector array (WCDA), and 18 wide field-of-view air Cherenkov/fluorescence telescopes (WFCTA)[12]. It will carry out accurate measurements of the EAS by employing hybrid detecting technologies mentioned above.

As the major array of LHAASO, KM2A is composed of 5195 EDs and 1188 MDs (as shown in figure1) [12,13].All the detectors are arranged in a triangular grid. The ED array is divided into two parts: a central part with 4901 EDs (15 m spacing) and a guard ring with 294 EDs (30 m spacing). The MDs are distributed in the central part of the array with a spacing of 30 m.

Even though the LHAASO construction is still ongoing, the installed detectors are already operational. By analyzing the KM2A data (with shower mode) from December 2019 to May 2020, Aharonian et al, presented the first observation of the Crab Nebula and tested the detector performance of KM2A array [2]. In order to broaden the energy range of the primary cosmic ray detected by LHAASO experiments, and push forward the work related the physics subjects in low energy region as soon as possible, it is urgent to carry out the studies on trigger setting of scaler mode.

PoS(ICRC2021)365

3. Simulation scheme and parameter setting of scaler mode

The simulation includes the EAS simulation and the detector response of the secondary particles. We simulated the evolution of EAS with CORSIKA [14] and analyzed the detector response by using G4KM2A [15]. G4KM2A, a specific software, based on GEANT4 package [16], can successfully simulate the response process of secondary particles passing through the KM2A detectors.

During the operation of the experiment, some detectors may malfunction, namely the experimental data may be abnormal. In the trigger setting of scaler mode, the whole array needs to be grouped into multiple detection units called "clusters". Before the data analysis, the abnormal "clusters" will be removed first to ensure the experimental data is reliable. In this paper, each ED cluster is made up of 64 EDs (8EDs × 8EDs), and a MD cluster consists of 16 MDs (4MDs × 4MDs)(as shown in figure1). The coincidence time is set to 100 ns and the event rates are recorded every 0.1 s.

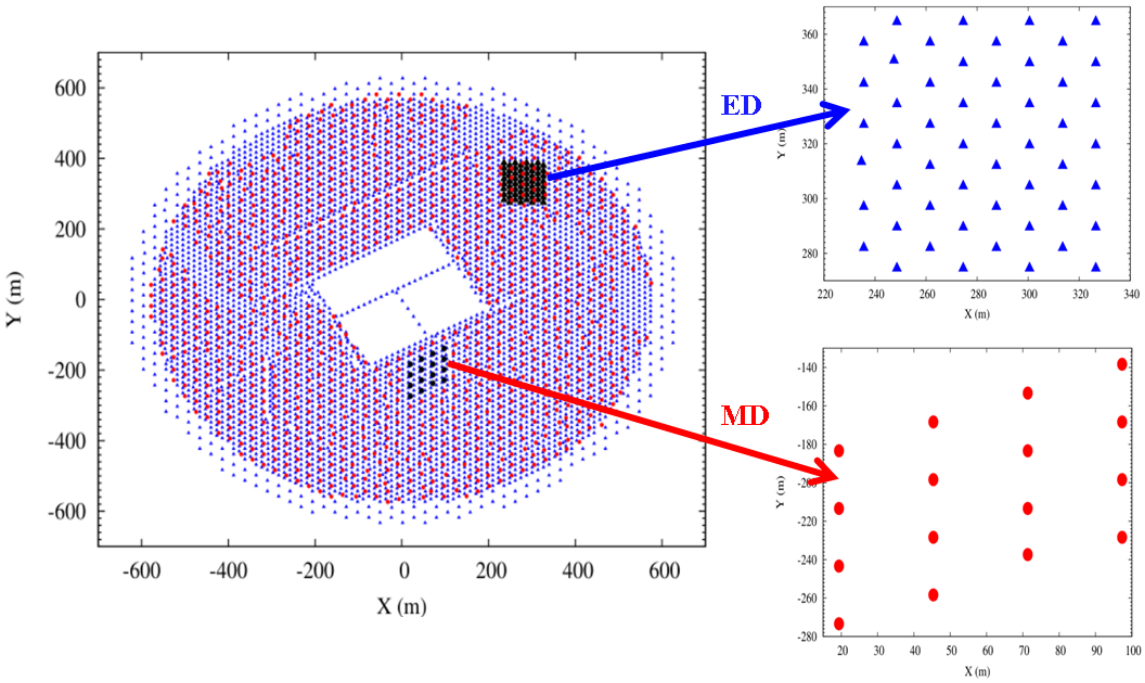

Figure 1: Layout diagram of KM2A array (left) and the cluster in scaler mode (right).

The specific simulation scheme of scaler mode is as follws:

1) Adopting the CORSIKA 7.5700 to study the cascade processes of extensive air showers in the atmosphere. The primary shower includes proton and helium nuclei in our simulations, with a zenith angle distributed from 0° to 70°, and the primary energy ranging from 14 GeV to 1000 TeV, following power-law function with spectral indexes of -2.7 and -2.64, respectively. QGSJETII-04 was used for the high-energy hadronic interactions while GHEISHA for the low energy ones. The energy cutoff is 0.5 MeV for positrons and electrons. According to the altitude of LHAASO station, the values of the geomagnetic field components used in this work are B_X = 34.6 μT, B_Z = 35.9 μT, for the horizontal and vertical intensity, respectively.

PoS(ICRC2021)365

2) Employing the G4KM2A to simulate the detector response in KM2A.

As we know, the shower events with core out of the array make a great contribution to low multiplicity events. To collect enough information about the secondary particles, the sample area in scaler mode should be sufficiently large when using G4KM2A to simulate the detector response.As shown in figure 2, the percentage of the detected particles increases rapidly with the increasing radius at first, and gradually reaches a constant value ~ 99.4% at a radius of 8000 m. In this case, it is thought that a circular region with a radius of 8000 m is an appropriate sample area in our simulations.

3) Sampling and merging the simulated data. First, the primary fluxes of proton and helium are calculated [17, 18], and the number of shower events in a fixed time is obtained by Poisson

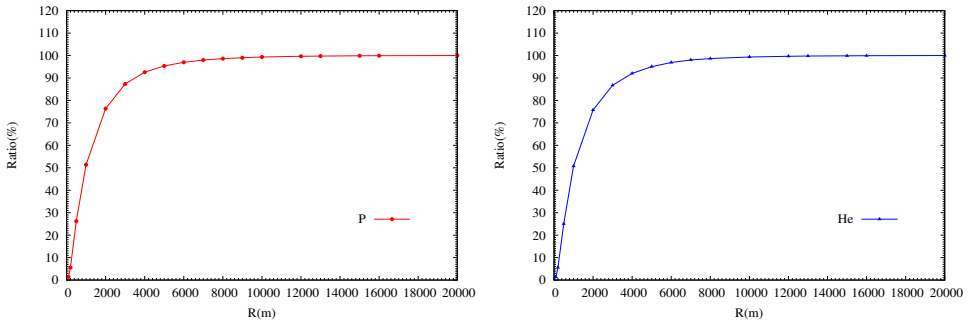

Figure 2: Percentage distribution of the detected particles as a function of sample radius.

distribution sampling. Then, the time intervals of these events are sampled using exponential distribution. Finally, according to the number and time of sampling, ranking the shower events after detector response, the simulated data similar to the experimental data are obtained.

4) Analyzing the simulating data. Here, the number of fired detectors in one cluster within the coincidence time is defined as multiplicity (m). For each cluster in ED array, there are four independent scaler channels to record the counting rates referred to multiplicities (m) $\geq$ 1, 2, 3 and 4, respectively, the same as each MD cluster.

4. Simulation results

4.1 The average counting rates for each ED/MD

By analyzing the experimental data of KM2A-ED array, the counting rate of an ED is ~ 1600 Hz. In general, the noise of the detector is in the range of 700 - 900 Hz. Following the simulation scheme in Section 3, we obtained simulation data of 6.0 s to statistic the counting rates for single ED/MD. Figure 3 shows the distribution of counting rates for one ED/MD. The average counting rates of one ED is ~ 750 Hz (~ 550 Hz for proton and ~ 200 Hz for helium). As for MD, the noise is not taking into account since it has little effects. The average counting rates for a MD is ~ 5300 Hz (~ 4060 Hz for proton and ~ 1240 Hz for helium). The simulation results are basically consistent with the experimental detections.

4.2 Simulation results of scaler mode in KM2A array

Here, we show the simulation results of scaler mode in ED and MD array, respectively.

PoS(ICRC2021)365

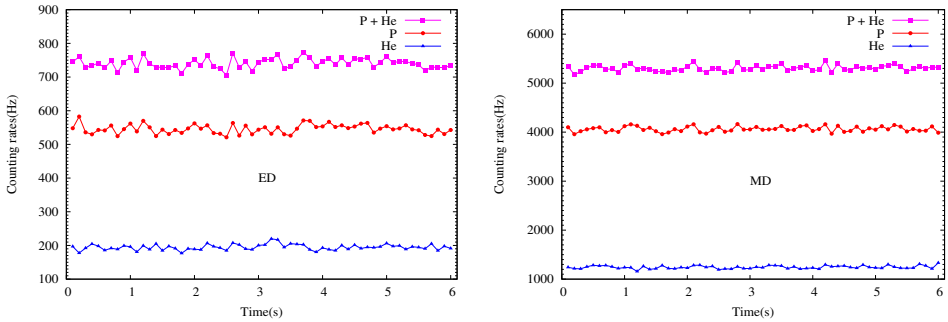

Figure 3: The distribution of counting rates for one ED/MD.

In order to statistics the counting rate of different multiplicities in an ED cluster, the noise is assumed to be 800 Hz and a fluctuation of randomly distribution is added. In the simulation, an ED cluster is composed of 64 EDs, and the coincidence time window is 100 ns. Figure 4 shows the distribution of counting rates with different multiplicities. The average rates of the four multiplicities (m) $\geq$ 1, 2, 3, and $\geq$4 are $\sim$ 88 kHz, $\sim$ 1.4 kHz, $\sim$ 210 Hz and $\sim$ 110 Hz, respectively. It decreases rapidly as the multiplicity increases.

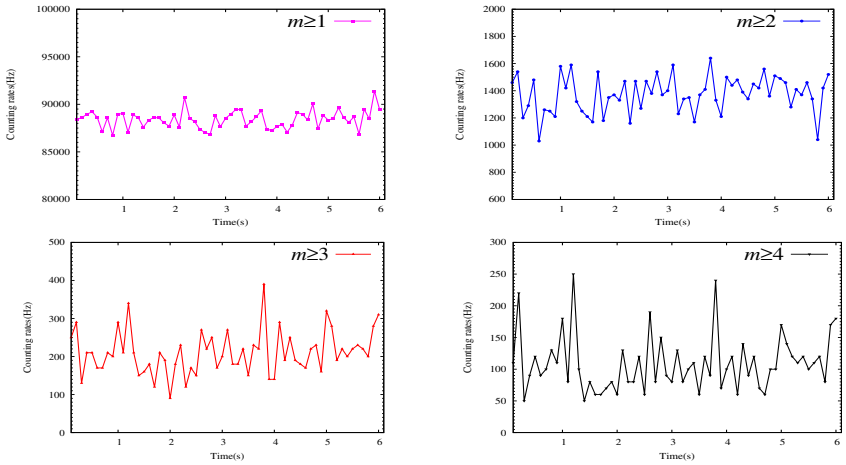

Figure 4: The distribution of counting rates for 64 EDs with $m \geq$ 1, 2, 3 and 4 in scaler mode.

In the ground cosmic ray experiments, the detector not only records the cosmic ray components, but also the background noise. So it is of great significance to quantify the contribution of cosmic ray particles to count rates with different multiplicities. According to the simulation, while $m \geq 1$, 2 , 3 and 4, the corresponding percentages of cosmic ray composition are $\sim$ 43.2%, $\sim$ 73.4%, $\sim$ 99.2% and $\sim$ 99.7%, respectively. It indicates that the contribution of cosmic rays increases with the multiplicity. When $m \geq 1$ and 2, more noise is recorded. It is worth noting that while $m \geq 3$, the particles recorded in scaler mode are almost completely due to cosmic rays.

In the simulation of KM2A-MD array, 16 MDs make up a detecting unit, with a time window of 100 ns. Due to the low noise of MD, only the event rates of $m \geq 1$ and 2 are counted. The distribution of counting rates for a MD cluster is shown in figure 5. The mean rates for $m \geq 1$ and 2 are $\sim$ 84 kHz and $\sim$ 890 Hz, respectively. To be different from ED, there is nearly no noise in MD, the records almost totally come from cosmic rays.

PoS(ICRC2021)365

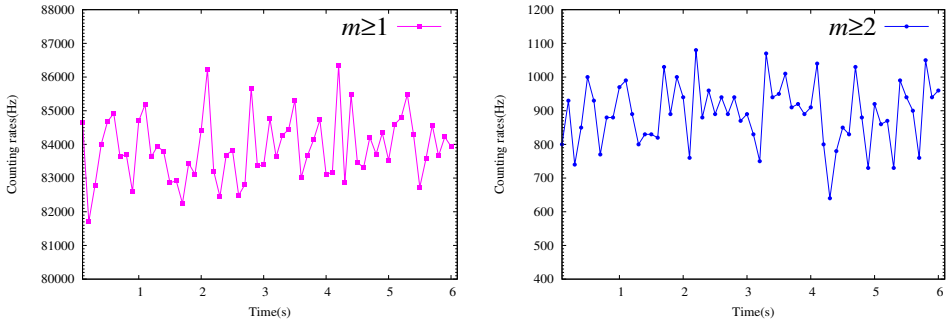

Figure 5: The distribution of counting rates for 16 MDs with $m \geq 1$ and 2 in scaler mode.

4.3 Simulation results of the threshold energy in KM2A array

Reducing the energy threshold of the detector is an important goal in ground-based cosmic ray experiments. In scaler mode, there is no need to satisfy the trigger conditions of the high multiplicity, the energy threshold for primary cosmic rays can be reduced. To compare the primary energy threshold, we studied the energy distributions of primary protons and helium of LHAASO-KM2A in scaler and shower mode by simulation.

By analyzing the simulation results in scaler mode, we found the energy threshold of primary cosmic ray particles is related to the multiplicity and the type of primary particles. The larger the multiplicity is, the greater the energy will be. As the multiplicity fixed, the energy threshold of primary protons is less than that of primary helium. The energy distributions of the two primary particles at $m \geq 1$ for ED/MD array are shown in figuer 6. The mean energies of the detected primary proton and helium are ~ 95 GeV and ~ 246 GeV. As for MD array, the corresponding mean energies of the primary proton is ~ 85 GeV and helium is ~ 316 GeV.

As for shower mode, the triggered proton and helium energy distributions for the full KM2A array are shown in figure 7. When the trigger threshold is set to 20 detectors fired within 400ns, the corresponding energy threshold for proton and helium are ~ 12.6 TeV and ~ 20 TeV, respectively.

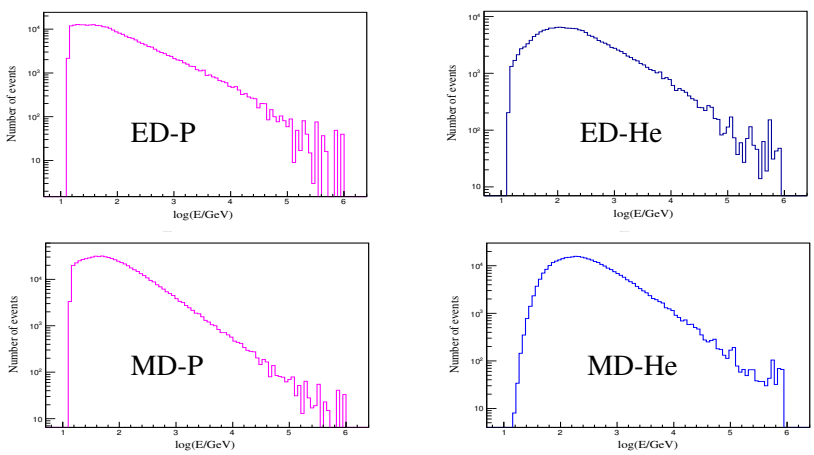

Figure 6: The energy distribution for primary proton and helium of scaler mode ($m \geq 1$) in KM2A array.

PoS(ICRC2021)365

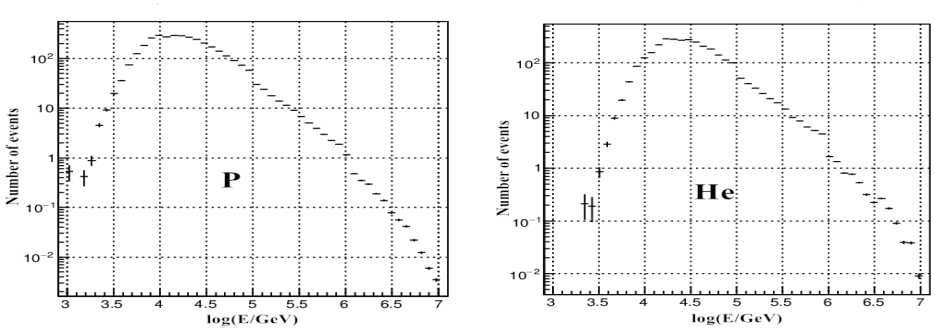

Figure 7: The trigger event energy of proton and helium of the full KM2A array.

Through contrastive analysis, it is clearly true that the detection threshold of scaler mode is lower than that of shower mode.

5. Conclusions

In this paper, the software packages CORSIKA and G4KM2A are used to simulate scaler mode in KM2A array. The main conclusions are drawn as follows:

1) An ED cluster is composed of 64 EDs, and the coincidence time window is 100 ns. The average rates of the four multiplicities (m) $\geq$ 1, 2, 3 and 4 are $\sim$ 88 kHz, $\sim$ 1.4 kHz, $\sim$ 210 Hz and $\sim$110 Hz, respectively. The contribution of cosmic rays increases with the increase of multiplicity. When $m \geq 3$, the count rates recorded in the scaler mode are almost exclusively cosmic rays.

2) A MD cluster consists of 16 MDs, the coincidence time window is also 100 ns. The average counting rates for $m \geq 1$ and 2 are $\sim$ 84 kHz and $\sim$ 890 Hz, respectively. There is almost no noise in MD, and the counting rates almost comes from cosmic rays.

3) It is found that the energy threshold of KM2A can be reduced by two orders of magnitude to 100 GeV when $m \geq 1$ in the scaler mode.

So far, the data acquisition mode applied in the LHAASO-KM2A experiment is only the shower mode. Our simulation results will provide specific scheme and parameter information for data triggering of scaler mode, and will give helpful references for follow-up data analysis in the LHAASO experiment.

6. Acknowledgments

This work is supported by the National Natural Science Foundation of China (NSFC) under Grants No. U2031101, 11475141 and 12047576, the National Key R&D Program of China under the grant No. 2018YFA0404201, and the Key Laboratory of Cosmic Ray of Tibet University Ministry of Education, Chia(Grant No. KLCR-202101)

References

[1] Bartoli B et al. 2017 *Astrophys. J.* **842** 31

[2] Aharonian F et al 2021 *Chinese Phys. C* **45** 025002

PoS(ICRC2021)365

[3] Di Girolamo T 2016 *Nucl. Part. Phys. Proc.* **279-281** 79-86

[4] Bartoli B et al. 2015 *Astrophys. J.* **806** 20

[5] Bartoli B et al 2015 *Phys. Rev. D* **92** 092005

[6] Vernetto S 2000 *Astropart. Phys.* **13** 75-86

[7] Aielli G et al. 2008 *Astropart. Phys.* **30** 85-95

[8] Bartoli B et al. 2014 *Astrophys. J.* **794** 82

[9] Dasso S et al. 2012 *Adv. Space Res.* **49** 1563-1569

[10] Bartoli B et al. 2018 *Phys. Rev. D* **97** 042001

[11] Zhou X X et al. 2015 *Acta Phys. Sin.* **64** 149202 (in Chinese)

[12] He H H 2018 *Radiation Detection Technology and Methods*, **2**, 1-8

[13] Cao Z et al. 2019 *Chinese Astron. Astr.* **43** 457-478

[14] Heck D et al. https://www.ikp.kit.edu/corsika/70.php [2021-04-08]

[15] Chen S Z et al. 2017 *Nuclear Electronicsetection Technology* **37(11)** 1101-1105 (in Chinese)

[16] Allison J et al. 2016 *Nucl. Instrum. Meth. A* **835** 186-225

[17] Aguilar M, Aisa D, Alpat B 2015 *Phys. Rev. Lett.* **114** 171103

[18] Aguilar M, Aisa D, Alpat B 2015 *Phys. Rev. Lett.* **115** 211101

PoS(ICRC2021)365

Full Authors List: LHAASO Collaboration

Zhen Cao[1,2,3], F. Aharonian[4,5], Q. An[6,7], Axikegu[8], L.X. Bai[9], Y.X. Bai[1,3], Y.W. Bao[10], D. Bastieri[11], X.J. Bi[1,2,3], Y.J. Bi[1,3], H. Cai[12], J.T. Cai[11], Zhe Cao[6,7], J. Chang[13], J.F. Chang[1,3,6], B.M. Chen[14], E.S. Chen[1,2,3], J. Chen[9], Liang Chen[1,2,3], Liang Chen[15], Long Chen[8], M.J. Chen[1,3], M.L. Chen[1,3,6], Q.H. Chen[8], S.H. Chen[1,2,3], S.Z. Chen[1,3], T.L. Chen[16], X.L. Chen[1,2,3], Y. Chen[10], N. Cheng[1,3], Y.D. Cheng[1,3], S.W. Cui[14], X.H. Cui[17], Y.D. Cui[18], B. D'Ettorre Piazzoli[19], B.Z. Dai[20], H.L. Dai[1,3,6], Z.G. Dai[7], Danzengluobu[16], D. della Volpe[21], X.J. Dong[1,3], K.K. Duan[13], J.H. Fan[11], Y.Z. Fan[13], Z.X. Fan[1,3], J. Fang[20], K. Fang[1,3], C.F. Feng[22], L. Feng[13], S.H. Feng[1,3], Y.L. Feng[13], B. Gao[1,3], C.D. Gao[22], L.Q. Gao[1,2,3], Q. Gao[16], W. Gao[22], M.M. Ge[20], L.S. Geng[1,3], G.H. Gong[23], Q.B. Gou[1,3], M.H. Gu[1,3,6], F.L. Guo[15], J.G. Guo[1,2,3], X.L. Guo[8], Y.Q. Guo[1,3], Y.Y. Guo[1,2,3,13], Y.A. Han[24], H.H. He[1,2,3], H.N. He[13], J.C. He[1,2,3], S.L. He[11], X.B. He[18], Y. He[8], M. Heller[21], Y.K. Hor[18], C. Hou[1,3], H.B. Hu[1,2,3], S. Hu[9], S.C. Hu[1,2,3], X.J. Hu[23], D.H. Huang[8], Q.L. Huang[1,3], W.H. Huang[22], X.T. Huang[22], X.Y. Huang[13], Z.C. Huang[8], F. Ji[1,3], X.L. Ji[1,3,6], H.Y. Jia[8], K. Jiang[6,7], Z.J. Jiang[20], C. Jin[1,2,3], T. Ke[1,3], D. Kuleshov[25], K. Levochkin[25], B.B. Li[14], Cheng Li[6,7], Cong Li[1,3], F. Li[1,3,6], H.B. Li[1,3], H.C. Li[1,3], H.Y. Li[7,13], J. Li[1,3,6], K. Li[1,3], W.L. Li[22], X.R. Li[1,3], Xin Li[6,7], Xin Li[8], Y. Li[9], Y.Z. Li[1,2,3], Zhe Li[1,3], Zhuo Li[26], E.W. Liang[27], Y.F. Liang[27], S.J. Lin[18], B. Liu[7], C. Liu[1,3], D. Liu[22], H. Liu[8], H.D. Liu[24], J. Liu[1,3], J.L. Liu[28], J.S. Liu[18], J.Y. Liu[1,3], M.Y. Liu[16], R.Y. Liu[10], S.M. Liu[8], W. Liu[1,3], Y. Liu[11], Y.N. Liu[23], Z.X. Liu[9], W.J. Long[8], R. Lu[20], H.K. Lv[1,3], B.Q. Ma[26], L.L. Ma[1,3], X.H. Ma[1,3], J.R. Mao[29], A. Masood[8], Z. Min[1,3], W. Mitthumsiri[30], T. Montaruli[21], Y.C. Nan[22], B.Y. Pang[8], P. Pattarakijwanich[30], Z.Y. Pei[11], M.Y. Qi[1,3], Y.Q. Qi[14], B.Q. Qiao[1,3], J.J. Qin[7], D. Ruffolo[30], V. Rulev[25], A. Saiz[30], L. Shao[14], O. Shchegolev[25,31], X.D. Sheng[1,3], J.Y. Shi[1,3], H.C. Song[26], Yu.V. Stenkin[25,31], V. Stepanov[25], Y. Su[32], Q.N. Sun[8], X.N. Sun[27], Z.B. Sun[33], P.H.T. Tam[18], Z.B. Tang[6,7], W.W. Tian[2,17], B.D. Wang[1,3], C. Wang[33], H. Wang[8], H.G. Wang[11], J.C. Wang[29], J.S. Wang[28], L.P. Wang[22], L.Y. Wang[1,3], R.N. Wang[8], W. Wang[18], W. Wang[12], X.G. Wang[27], X.J. Wang[1,3], X.Y. Wang[10], Y. Wang[8], Y.D. Wang[1,3], Y.J. Wang[1,3], Y.P. Wang[1,2,3], Z.H. Wang[9], Z.X. Wang[20], Zhen Wang[28], Zheng Wang[1,3,6], D.M. Wei[13], J.J. Wei[13], Y.J. Wei[1,2,3], T. Wen[20], C.Y. Wu[1,3], H.R. Wu[1,3], S. Wu[1,3], W.X. Wu[8], X.F. Wu[13], S.Q. Xi[1,3], J. Xia[7,13], J.J. Xia[8], G.M. Xiang[2,15], D.X. Xiao[16], G. Xiao[1,3], H.B. Xiao[11], G.G. Xin[12], Y.L. Xin[8], Y. Xing[15], D.L. Xu[28], R.X. Xu[26], L. Xue[22], D.H. Yan[29], J.Z. Yan[13], C.W. Yang[9], F.F. Yang[1,3,6], J.Y. Yang[18], L.L. Yang[18], M.J. Yang[1,3], R.Z. Yang[7], S.B. Yang[20], Y.H. Yao[9], Z.G. Yao[1,3], Y.M. Ye[23], L.Q. Yin[1,3], N. Yin[22], X.H. You[1,3], Z.Y. You[1,2,3], Y.H. Yu[22], Q. Yuan[13], H.D. Zeng[13], T.X. Zeng[1,3,6], W. Zeng[20], Z.K. Zeng[1,2,3], M. Zha[1,3], X.X. Zhai[1,3], B.B. Zhang[10], H.M. Zhang[10], H.Y. Zhang[22], J.L. Zhang[17], J.W. Zhang[9], L.X. Zhang[11], Li Zhang[20], Lu Zhang[14], P.F. Zhang[20], P.P. Zhang[14], R. Zhang[7,13], S.R. Zhang[14], S.S. Zhang[1,3], X. Zhang[10], X.P. Zhang[1,3], Y.F. Zhang[8], Y.L. Zhang[1,3], Yi Zhang[1,13], Yong Zhang[1,3], B. Zhao[8], J. Zhao[1,3], L. Zhao[6,7], L.Z. Zhao[14], S.P. Zhao[13,22], F. Zheng[33], Y. Zheng[8], B. Zhou[1,3], H. Zhou[28], J.N. Zhou[15], P. Zhou[10], R. Zhou[9], X.X. Zhou[8], C.G. Zhu[22], F.R. Zhu[8], H. Zhu[17], K.J. Zhu[1,2,3,6], and X. Zuo[1,3].

[1]Key Laboratory of Particle Astrophyics & Experimental Physics Division & Computing Center, Institute of High Energy Physics, Chinese Academy of Sciences, 100049 Beijing, China.
[2]University of Chinese Academy of Sciences, 100049 Beijing, China.
[3]TIANFU Cosmic Ray Research Center, Chengdu, Sichuan, China.
[4]Dublin Institute for Advanced Studies, 31 Fitzwilliam Place, 2 Dublin, Ireland.
[5]Max-Planck-Institut for Nuclear Physics, P.O. Box 103980, 69029 Heidelberg, Germany.
[6]State Key Laboratory of Particle Detection and Electronics, China.
[7]University of Science and Technology of China, 230026 Hefei, Anhui, China.
[8]School of Physical Science and Technology & School of Information Science and Technology, Southwest Jiaotong University, 610031 Chengdu, Sichuan, China.
[9]College of Physics, Sichuan University, 610065 Chengdu, Sichuan, China.
[10]School of Astronomy and Space Science, Nanjing University, 210023 Nanjing, Jiangsu, China.
[11]Center for Astrophysics, Guangzhou University, 510006 Guangzhou, Guangdong, China.
[12]School of Physics and Technology, Wuhan University, 430072 Wuhan, Hubei, China.
[13]Key Laboratory of Dark Matter and Space Astronomy, Purple Mountain Observatory, Chinese Academy of Sciences, 210023 Nanjing, Jiangsu, China.
[14]Hebei Normal University, 050024 Shijiazhuang, Hebei, China.
[15]Key Laboratory for Research in Galaxies and Cosmology, Shanghai Astronomical Observatory, Chinese Academy of Sciences, 200030 Shanghai, China.
[16]Key Laboratory of Cosmic Rays (Tibet University), Ministry of Education, 850000 Lhasa, Tibet, China.
[17]National Astronomical Observatories, Chinese Academy of Sciences, 100101 Beijing, China.
[18]School of Physics and Astronomy & School of Physics (Guangzhou), Sun Yat-sen University, 519000 Zhuhai, Guangdong, China.
[19]Dipartimento di Fisica dell'Universit'a di Napoli "Federico II", Complesso Universitario di Monte Sant'Angelo, via Cinthia, 80126 Napoli, Italy.
[20]School of Physics and Astronomy, Yunnan University, 650091 Kunming, Yunnan, China.
[21]D'epartement de Physique Nucl'eaire et Corpusculaire, Facult'e de Sciences, Universit'e de Gen'eve, 24 Quai Ernest Ansermet, 1211 Geneva, Switzerland
[22]Institute of Frontier and Interdisciplinary Science, Shandong University, 266237 Qingdao, Shandong, China.
[23]Department of Engineering Physics, Tsinghua University, 100084 Beijing, China.
[24]School of Physics and Microelectronics, Zhengzhou University, 450001 Zhengzhou, Henan, China.
[25]Institute for Nuclear Research of Russian Academy of Sciences, 117312 Moscow, Russia.

PoS(ICRC2021)365

[26]School of Physics, Peking University, 100871 Beijing, China.
[27]School of Physical Science and Technology, Guangxi University, 530004 Nanning, Guangxi, China.
[28]Tsung-Dao Lee Institute & School of Physics and Astronomy, Shanghai Jiao Tong University, 200240 Shanghai, China.
[29]Yunnan Observatories, Chinese Academy of Sciences, 650216 Kunming, Yunnan, China.
[30]Department of Physics, Faculty of Science, Mahidol University, 10400 Bangkok, Thailand.
[31]Moscow Institute of Physics and Technology, 141700 Moscow, Russia.
[32]Key Laboratory of Radio Astronomy, Purple Mountain Observatory, Chinese Academy of Sciences, 210023 Nanjing, Jiangsu, China.
[33]National Space Science Center, Chinese Academy of Sciences, 100190 Beijing, China.

PoS(ICRC2021)365